Princeton Plasma Physics Laboratory

PPPL- 4961

PPPL- 4961

Emission Processes at the Deposit in the Carbon Arc Discharge for Nanotube Synthesis

J. Ng and Y. Raitses

DECEMBER, 2013

PPPL PRINCETON PLASMA PHYSICS LABORATORY

Prepared for the U.S. Department of Energy under Contract DE-AC02-09CH11466.

Princeton Plasma Physics Laboratory
Report Disclaimers

Full Legal Disclaimer

Trademark Disclaimer

PPPL Report Availability

Princeton Plasma Physics Laboratory:

http://www.pppl.gov/techreports.cfm

Office of Scientific and Technical Information (OSTI):

http://www.osti.gov/bridge

Related Links:

U.S. Department of Energy

Office of Scientific and Technical Information

Fusion Links

Emission Processes at the deposit in the Carbon Arc Discharge for nanotube synthesis

J. Ng and Y. Raitses
Princeton Plasma Physics Laboratory, Princeton, NJ 08540
(Dated: October 29, 2013)

The atmospheric pressure carbon arc in helium is an important method for nanotube production. Typical arcs operate in a dc mode between a graphite anode, which is consumed, and a cathode which may be a lower melting point material. It is accepted that electrons from the cathode are emitted by thermionic field emission, requiring the cathode to be above the melting temperature of its material. However, the cathode usually remains undamaged by the arc, raising the question about how the electron current in the arc is supported. Our experiments with copper and graphite cathodes have demonstrated that a sufficiently large area of the cathode is hot enough for thermionic emission to be the source of most of the arc current, but emission is from the carbon deposit formed on the cathode during arc operation. Due to its low heat conductivity, the cathode does not reach its melting point and remains undamaged.

I. INTRODUCTION

Since their discovery in the early 19$^{\text{th}}$ century [1], carbon arcs have been used as radiation standards [2], in image furnaces [3] and in carbon arc welding among other things. More recently, they have been used as an efficient method for the production of high purity carbon nanotubes [4–6], in which the graphite anode ablates and nanotubes and other fullerines are formed in a deposit on the cathode surface [5, 7]. Due to their unique electrical and mechanical properties [8–10], nanotubes could potentially be used for hydrogen storage, nanoelectronics, chemical sensors and many other applications [8, 9].

Although the initial discovery used graphite for both cathode and anode [4], and this setup is commonly used [5, 11, 12], Colbert et. al. [7] found that using a water cooled copper cathode reduced sintering in the nanotubes formed in the deposit, while other workers have used cathodes of material such as copper and stainless steel [13–15].

The use of low melting point cathodes (copper melts at 1085 °C compared to graphite which sublimes at 3642 °C) raises a basic question about the operation of the arc, namely how electrons are emitted from the cathode. While this has been studied in detail for cathodic arcs [16–20], the arc used in nanosynthesis is an anodic arc and operates in a different regime. The model in Ref. [21] shows that temperatures over 3000 °C are required at the cathode, while experimentally, cathodes remain undamaged during the process.

To explain this discrepancy, the current density at the cathode could be reduced by having the current flow to the entire cathode surface, reducing the temperature required for thermionic emission to support the current, which has been observed in simulations [11]. Alternatively, it has been proposed that the deposit formed during the arc is the source of emission based on its structure after arc operation [22]. This is supported by observations that carbon-copper arcs became carbon-carbon arcs after deposit formation on the copper electrode [23].

In order to determine the source of electrons in the arc and the current distribution at the cathode, we operate the carbon arc using different cathode geometries, together with in-situ and infrared temperature measurements. Our results show that during the steady state operation of the arc, most of the current flows within the area directly across from and of similar size to the anode, and that the formation of the deposit plays an important role in electron emission. The deposit 1) reaches the high temperatures necessary for thermionic emission to provide the electron current, 2) reduces heat flux to the copper cathode and 3) changes the arc from graphite-copper or graphite-graphite to graphite-deposit.

II. EXPERIMENTAL SETUP

The arc experiments were performed in a helium atmosphere within a 10 inch 6-way cross using the setup shown in Figure 1, which is similar to that used in Refs. [13, 24]. The helium pressure was maintained at 500 Torr using a computer-controlled solenoidal valve. Cylindrical graphite anodes and cathodes of diameter 6 mm and 12 mm were used, where 6 mm is the typical anode diameter in synthesis experiments [5, 7, 25]. The copper cathodes had diameters 38 mm and 50 mm.

The position of the anode was controlled by a stepper motor and a potentiometer used to measure the arc voltage, both connected to a data acquisition system. In all the experiments performed, the electrode separation was controlled by maintaining the discharge voltage between 20 and 25 V as the anode ablated. Discharge current was kept between 50 and 80 A. Arcing was initiated by bringing the anode into contact with the cathode, after which the control system would increase the electrode separation until the specified arc voltage was reached.

To measure the cathode temperature, a K-type thermocouple was placed 2 mm below the surface of a copper cathode directly opposite the anode. Experiments to measure the deposit temperature used an electrode in which existing cathode deposits to be mounted (Fig. 2), and a C-type thermocouple was placed just below the surface of the deposit. Additionally, a FLIR Tau 640 1.7 infrared camera together with a 3.2% transmittance

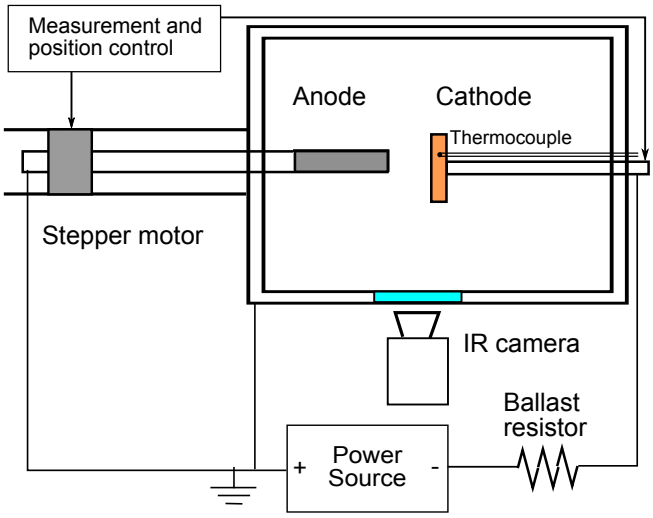

FIG. 1. Setup used in carbon arc experiments, similar to Ref. [13].

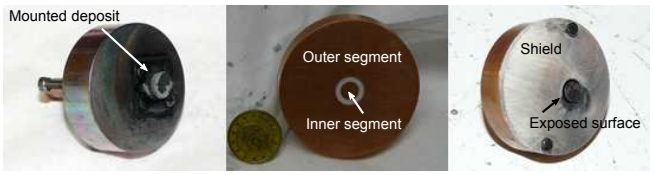

FIG. 2. Cathodes used in the experiment. From left to right, copper cathode with mounted deposit, segmented cathode, shielded cathode.

neutral density filter was used for temperature measurements. Absolute calibration of the camera was performed using arcs between graphite electrodes in conjunction with thermocouple measurements.

For the experiments used to determine the current distribution in the arc, shielded and segmented cathodes were used with 6 mm graphite anodes. The shielded copper cathode was covered by an insulating layer of boron-nitride except for a 6 mm diameter opening, while the segmented cathode consisted of an inner region of 6 mm diameter insulated from an outer ring of diameter 50 mm by a 2 mm layer of insulation.

III. ELECTRON EMISSION

We now analyse possible mechanisms of electron emission which could supply the electrons necessary to maintain the current observed in arcs. To do so, we first estimate the electron current fraction by measuring the ablation rates for 65 A arcs, and show that the current cannot be supported by emission from the copper surface. Under the conditions described in the previous section, the arcs operated in the anodic mode with deposit formation on the cathode [13, 25]. The results are shown in Table I and are consistent with measurements by Fetterman *et. al.* No appreciable difference between the rates for copper and carbon cathodes was observed [13]. The deposits grown were roughly circular with diameter 6-7 mm. With the 6 mm diameter anodes, deposits would grow until the extinguishing of the arc (in this set of experiments the longest was 17 mm), while with the 12 mm diameter anodes deposits were 1 mm thick.

The maximum ion current is estimated by assuming that all the ablated material is singly ionised and delivers current to the cathode. To account for current due to evaporation from the cathode and redeposition [26, 27], we assume that the evaporation rate at the cathode is less than that at the anode. If all of the evaporated atoms at the cathode were ionised and redeposited, the total ion current would be twice that due to ions from the anode. The resulting current is shown in the final column of Table I. For the 12 mm anode, an electron current of larger than 60 A would be required to support the arc. For the 6 mm anode, the observed ablation could support the arc current; however, in a typical carbon arc, the ionisation degree is 10^{-3} to 10^{-4}, much less than the 100% assumed here [28]. The ion current would then be reduced to less than 0.12 A, so we would also expect a large electron current for the 6 mm anode.

Cathode	Anode diameter (mm)	Ablation (mg/s)	Max ion current (A)
Carbon	12 mm	0.33 ± 0.12	5.2 ± 1.9
Carbon	6 mm	8 ± 2	128 ± 32
Copper	12 mm	0.33 ± 0.08	5.2 ± 1.2
Copper	6 mm	10 ± 2	160 ± 32

TABLE I. Ablation rates and estimated ion current for a 65 A arc with different cathode materials and anode diameters.

Supplying this electron current requires electron emission from the cathode, which can take the form of thermo-field emission, secondary emission or photoemission [1, 16, 29]. In particular, Ref. [29] shows that field emission and various ionisation mechanisms cannot account for the electron current observed in an argon arc with a non-thermionic cathode, and we perform a similar analysis for the carbon arc in helium.

A. Thermo-field emission

Heating a solid to high temperatures increases the number of electrons with the energy needed to overcome the work function, while strong electric fields at the surface modify the shape of the potential well. Electron emission due to the combination of these effects is known as thermo-field emission [16, 30, 31]. A parameterisation of the thermo-field current in units of A/cm^2 is given by Hantzsche [30]

$$j_{TF} = k(AT^2 + BE^{9/8}) \exp\left[-\left(\frac{T^2}{C} + \frac{E^2}{D}\right)^{-1/2}\right] \quad (1)$$

where $k = 1.45$, $A = 120$, $B = 406\ E^{0.1(\phi-4.5)} \exp(-2.22(\phi - 4.5))$, $C = 2.727 \times 10^9(\phi/4.5)^2$ and $D = 4.252 \times 10^{17}(\phi/4.5)^2$. T is the temperature in K, E the electric field in V/cm and ϕ the work function in eV.

With respect to our experiments, the current density was estimated as at least ~ 230 A/cm^2 for a 65 A arc with an electron current fraction of greater than 0.9, which would require temperatures of above 3200°C – above the melting point of copper – or electric fields of greater than 10^7 V/cm. If these conditions were to hold, there would be visible damage to the cathode due to melting and/or ablation, which we do not observe, or an unrealistic potential drop of the entire discharge voltage over 20 nm or less, which is much smaller than the Debye length of more than 180 nm, assuming a plasma density of $< 10^{21}$ m^{-3} and an estimated electron temperature of 0.6 eV close to the cathode [29, 32]. As such, thermo-field emission from the copper cathode cannot account for the observed electron emission during the steady state operation of the arc. Note that during the initial phase of the arc, it operates in the cathodic mode before a transition to the anodic mode which is studied here [28].

B. Secondary emission

Electrons are also emitted due to the bombardment of the surface by ions and excited atoms. In the carbon arc, only carbon ions are considered due to helium's high ionisation potential [11], though metastable helium atoms are present and can cause Auger emission[28, 33]. At low energies, the secondary electron yield γ_i from ion bombardment depends only on the ionisation energy I and work function ϕ and can be estimated by the empirical formula $\gamma_i = 0.016(I - 2e\phi)$ [1, 34]. For carbon ions impacting a copper surface, this is approximately 0.04. Given the ion current fraction of less than 0.1 in our experiment with the 12 mm anode, secondary emission due to ions provides at most 0.2 A for a 65 A arc and cannot be the source of the electrons in the arc.

In Ref. [29], Auger emission due to metastable excited argon atoms the main source of electron current [29]. For helium atoms and copper surfaces, the electron yield is about 1 electron per incident atom [35]. However, due to the higher excitation energies of helium and low arc voltage, the metastable density is too low to provide the required current. The density is found by balancing production by electron excitation against cumulative ionisation [33], given by

$$n_N n_e C_M^0 = n_M n_e C_M^+. \quad (2)$$

Here n_N is the neutral density, n_e the electron density and n_M is the metastable density. The C's are rate coefficients which are found by integrating the cross sections for excitation and ionisation with the electron distribution, assumed to be Maxwellian [33]. At an electron temperature of 0.6 eV, the estimated metastable helium density is on the order of 10^{11} m^{-3}, which gives a current of 13nA assuming thermal flux to the cathode. Auger emission due to carbon are not considered as the metastable ^{1}D and ^{1}S states have energies 1.3 eV and 2.7 eV, below the work functions of copper and graphite [36, 37].

C. Photoemission

To estimate the maximum photoemission from the surface, we assume that at most half of the radiation from the arc reaches the cathode, and a photon energy of 5 eV, the lowest wavelength line of carbon, which gives a yield of 10^{-2} electrons per photon at a copper surface [38, 39]. If all of the arc's power were radiated, 825 W of radiation would be available for photoemission, which would give a maximum current of approximately 1.7 A. The yield for graphite is approximately 10^{-6}, which would provide 1.7×10^{-4} A [40].

We have thus shown that the above emission mechanisms cannot account for the electron current from a low melting point cathode during an anodic arc. Instead, temperature measurements will reveal that it is the formation of the carbon deposit on the cathode which allows the high temperatures necessary for electron emission to be reached.

IV. CURRENT DISTRIBUTION AND CATHODE TEMPERATURE

To determine if the arc current flows through the entire cathode or just a small region, experiments with shielded and segmented cathodes were performed. In the experiment with the shielded cathode, a carbon deposit formed over the unshielded area, after which the arc continued to operate with the entire current flowing through the cathode deposit. With the segmented cathode, at most 4 A flowed through the outer segment during a 65 A arc. At lower currents, no current in the outer segment was observed. This shows that most of the current flows through the small central region directly opposite the anode. As such, the observed current density is over 230 A/cm^2. The observation that the arc operates between the deposit and anode is also consistent with Upson's [23] observations that the copper-carbon arc becomes the carbon-carbon arc after deposit formation.

The variation of copper cathode temperature with time for arcs with 12 mm and 6mm diameter anodes respectively is shown in Fig. 3. The highest temperature measured in the copper electrode was 1000 ± 20°C during the experiment with the larger anode, which is still below the melting point of copper of 1085°C. This was due to the cathode deposit being thinner, so that the thermocouple was in closer proximity to the actual cathode surface. Also of note in Fig. 3(b) is the extinguishing of the arc around $t = 100$ s and re-ignition at $t = 120$ s, caused by the deposit becoming detached from the cathode and falling off. Immediately after re-ignition, the rate of in-

crease of temperature was larger than just before $t = 100$ s, showing that the presence of the deposit reduces heat flux to the cathode. These observations show that the deposit is a critical element in the operation of the arc.

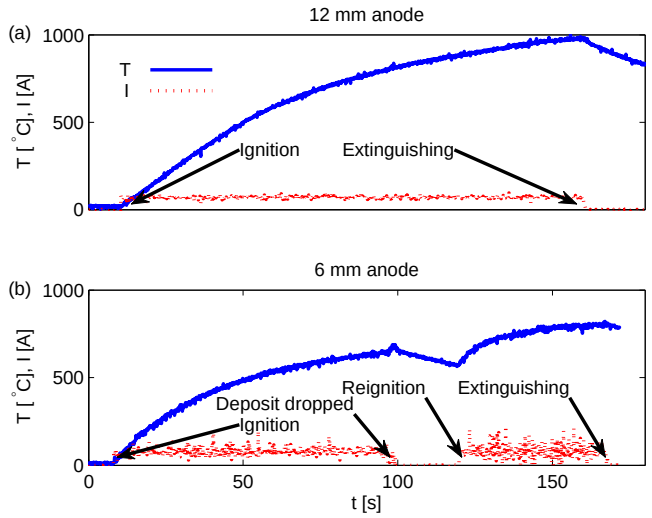

FIG. 3. Cathode temperature and discharge current during the operation of arcs with (a) 12 mm and (b) 6 mm anodes. The thermocouple was placed 2 mm below the cathode surface exposed to the arc.

Figure 4 shows infrared images of the electrodes during an arcs between 12 mm diameter anodes and graphite and copper cathodes. During both arcs, small deposits formed on the cathode, and the highest surface temperature was (3500 ± 200) K, with a larger region where temperatures were over 3100 K. The uncertainties in the temperature measurements are due to the extrapolation of the calibration curve. Thermocouple readings within the deposit were consistent with the infrared measurements and exceeded 2593 K, the maximum temperature which can be measured by C-type thermocouples. Data for 6 mm diameter anodes are not available due to the growth of the "collar" around the deposit preventing a clear view of its surface from being obtained. These results show that the deposit reaches the high temperatures necessary for thermionic emission to provide the electron current in the arc, in agreement with observations of the deposit structure after the arc [22]. Within the observed surface temperature range, the thermo-field emission current is between 60 and 500 A/cm^2, with most of the contribution being thermionic. This would supply at least a quarter to all of the current in the arc.

The deposit is thus the source of electron emission and is effectively the cathode, meaning that the arc should not be considered graphite-copper, but graphite-deposit [22, 23]. This also explains why the cathode remains undamaged, as the deposit reduces heat flux to the copper surface, as seen earlier in Fig. 3(b). It is known from Raman spectroscopy that its structure is different from graphite [24], and while data are not available for the deposit's thermal conductivity, the upper image in Fig. 4 shows that it is lower than that of graphite. Additionally, the known conductivity value for graphite is approximately 13 W/m/K above 2500 °C [41], which is already lower than that of copper, which is over 300 W/m/K above 1000 °C [42]. As such, the lower conductivity of the deposit allows a large temperature gradient exists across the deposit, which lets the metal cathode to remain below its melting temperature while the deposit emits electrons.

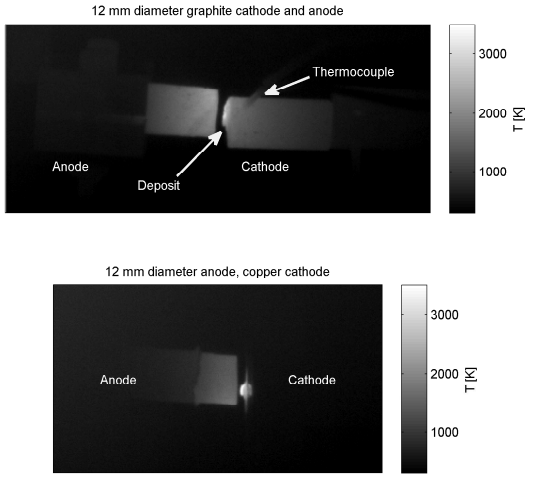

FIG. 4. Top: Infrared camera image of electrodes during an arc discharge between two 12 mm graphite electrodes. Bottom: Electrodes during arc between 12 mm graphite anode and copper cathode.

The results of our experiments reveal that the arc current flows through a small region opposite the anode and that thermionic emission is the source of electron emission during the anodic arc and explain how the high temperatures required for this process are reached without damaging the low-melting point cathode material. Due to the estimated low heat conductivity of the deposit, the high temperatures at the surface exposed to the arc required to support emission can exist without the cathode reaching its melting temperature. It should also be emphasized that the deposit also forms in experiments with graphite cathodes, meaning that the role of the deposit in the arc described here is more general and not exclusive to arcs with low melting point cathodes. Thus, after the formation of the deposit, the arc is not between the graphite anode and the cathode material, but is a graphite-cathode deposit arc. With respect to nanosynthesis, the growth of single-walled nanotubes mainly takes place on the periphery of the deposit [5, 11, 12], away from the region where the current flows, implying that the cathode material not covered by the deposit (in our case copper) is important in their formation [7].

V. CONCLUSION

To summarise, anodic arc experiments were conducted between graphite anodes and graphite and copper cathodes. For currents below 65 A, all of the current was found to flow within a 6 mm diameter region of the cathode directly opposite the anode, and is largely due to electrons. The formation of the cathode deposit is essential in the sustaining of the arc during steady state operation as it allows the high temperatures necessary for thermionic emission to provide the electron current in the arc to exist without damaging the cathode [22]. In addition, it changes the arc from a graphite-cathode to a graphite-deposit arc [23]. The formation of the deposit is not included in current models of the anodic arc for nanosynthesis [11, 21] and should be taken into consideration for a self-consistent model of the arc to be developed.

We would like to thank A. Merzhevskiy, E. Merino and M. Eagles for technical support, T. Gray for assisting with infrared measurements, M. Keidar and E. Türköz for fruitful discussions. This work was supported by DOE contract DE-AC02-09CH11466.

[1] Y. Raizer, *Gas Discharge Physics* (Springer-Verlag, 1991).
[2] M. R. Null and W. W. Lozier, J. Opt. Soc. Am. **52**, 1156 (1962).
[3] M. R. Null and W. W. Lozier, Review of Scientific Instruments **29**, 163 (1958).
[4] S. Iijima *et al.*, nature **354**, 56 (1991).
[5] C. Journet, W. Maser, P. Bernier, A. Loiseau, M. L. De La Chapelle, d. l. S. Lefrant, P. Deniard, R. Lee, and J. Fischer, Nature **388**, 756 (1997).
[6] A. Mansour, M. Razafinimanana, M. Monthioux, M. Pacheco, and A. Gleizes, Carbon **45**, 1651 (2007).
[7] D. T. Colbert, J. Zhang, S. M. McClure, P. Nikolaev, Z. Chen, J. H. Hafner, D. W. Owens, P. G. Kotula, C. B. Carter, J. H. Weaver, A. G. Rinzler, and R. E. Smalley, Science **266**, 1218 (1994), http://www.sciencemag.org/content/266/5188/1218.full.pdf.
[8] M. Keidar, A. Shashurin, J. Li, O. Volotskova, M. Kundrapu, and T. S. Zhuang, Journal of Physics D: Applied Physics **44**, 174006 (2011).
[9] R. H. Baughman, A. A. Zakhidov, and W. A. de Heer, Science **297**, 787 (2002), http://www.sciencemag.org/content/297/5582/787.full.pdf.
[10] E. T. Thostenson, Z. Ren, and T.-W. Chou, Composites Science and Technology **61**, 1899 (2001).
[11] M. Kundrapu and M. Keidar, Physics of Plasmas **19**, 073510 (2012).
[12] A. Ostrogorsky and C. Marin, Heat and Mass Transfer **42**, 470 (2006).
[13] A. J. Fetterman, Y. Raitses, and M. Keidar, Carbon **46**, 1322 (2008).
[14] V. Kresin and A. Aharony, Nature **377**, 135 (1995).
[15] M. Keidar, I. Levchenko, T. Arbel, M. Alexander, A. M. Waas, and K. K. Ostrikov, Applied Physics Letters **92**, 043129 (2008).
[16] A. Anders, *Cathodic arcs: From Fractal Spots to Energetic Condensation* (Springer, 2008).
[17] B. Jüttner, Journal of Physics D: Applied Physics **34**, R103 (2001).
[18] J.-L. Meunier and S. Coulombe, Pure Appl. Chem **70**, 1175 (1998).
[19] E. Hantzsche, in *Handbook of Vacuum Arc Science and Technology*, edited by R. L. Boxman, D. M. Sanders, and P. J. Martin (William Andrew Publishing, Park Ridge, NJ, 1996) pp. 151 – 208.
[20] M. S. Benilov and A. Marotta, Journal of Physics D: Applied Physics **28**, 1869 (1995).
[21] M. Keidar and I. I. Beilis, Journal of Applied Physics **106**, 103304 (2009).
[22] D. Tang, L. Sun, J. Zhou, W. Zhou, and S. Xie, Carbon **43**, 2812 (2005).
[23] W. L. Upson, Proceedings of the Physical Society of London **21**, 1 (1907).
[24] Y. Raitses, C. Skinner, F. Jiang, and T. Duffy, Journal of Nuclear Materials **375**, 365 (2008).
[25] A. Shashurin and M. Keidar, Carbon **46**, 1826 (2008).
[26] I. Beilis, IEEE Transactions on Plasma Science **34**, 855 (2006).
[27] V. F. Puchkarev and S. M. Chesnokov, Journal of Physics D: Applied Physics **25**, 1760 (1992).
[28] A. Shashurin, J. Li, T. Zhuang, M. Keidar, and I. I. Beilis, Physics of Plasmas **18**, 073505 (2011).
[29] J. Lowke and M. Tanaka, in *Gas Discharges and Their Applications, 2008. GD 2008. 17th International Conference on* (2008) pp. 137–140.
[30] E. Hantzsche, Beitrge aus der Plasmaphysik **22**, 325 (1982).
[31] E. L. Murphy and R. H. Good, Phys. Rev. **102**, 1464 (1956).
[32] Z. Markovic, B. Todorovic-Markovic, M. Marinkovic, and T. Nenadovic, Carbon **41**, 369 (2003).
[33] D. Korzec, M. R. Talukder, and M. Kando, Science and Technology of Advanced Materials **2**, 595 (2001).
[34] E. Cawthron, Australian Journal of Physics **24**, 859 (1971).
[35] F. B. Dunning and A. C. H. Smith, Journal of Physics B: Atomic and Molecular Physics **4**, 1696 (1971).
[36] P. S. Skell and R. R. Engel, Journal of the American Chemical Society **88**, 3749 (1966), http://pubs.acs.org/doi/pdf/10.1021/ja00968a014.
[37] R. S. Freund, The Journal of Chemical Physics **54**, 3125 (1971).
[38] C. N. Berglund and W. E. Spicer, Phys. Rev. **136**, A1044 (1964).
[39] A. Kramida, Y. Ralchenko, J. Reader, and NIST ASD Team, NIST Atomic Spectra Database (version 5.0) (2012).
[40] E. Taft and L. Apker, Phys. Rev. **99**, 1831 (1955).
[41] R. W. Powell and F. H. Schofield, Proceedings of the Physical Society **51**, 153 (1939).
[42] R. W. Powell, C. Y. Ho, and P. E. Liley, National Standard Reference Data Series - National Bureau of Stan-

dards **8** (1966).

The Princeton Plasma Physics Laboratory is operated
by Princeton University under contract
with the U.S. Department of Energy.

Information Services
Princeton Plasma Physics Laboratory
P.O. Box 451
Princeton, NJ 08543

Phone: 609-243-2245
Fax: 609-243-2751
e-mail: pppl_info@pppl.gov
Internet Address: http://www.pppl.gov